J. Astrophys. Astr. (2019) 40:20
https://doi.org/10.1007/s12036-019-9586-1

Impact of light pollution on the visibility of astronomical objects in medium-sized cities in Central Europe on the example of the city of Rzeszów, Poland

M. WESOŁOWSKI

Faculty of Mathematics and Natural Sciences, University of Rzeszów, Pigonia 1 Street, 35-310 Rzeszów, Poland.
E-mail: marwes@ur.edu.pl

MS received 20 December 2018; accepted 2 April 2019; published online 4 June 2019

Abstract. This paper discusses the influence of light pollution of the night sky on the conditions of visibility of astronomical objects such as planets, stars and comets. This phenomenon has a huge impact on the observability of astronomical objects, especially in cities, where the brightness of the sky makes it difficult or even impossible to conduct astronomical observations. The main purpose of this article is to measure and analyse the surface brightness of the night sky in Rzeszów and its surroundings. A device called the Sky Quality Meter was used to measure the brightness of the night sky. This paper presents measurement results for the years 2015 and 2018, from which it is clear that the quality of the night sky has been deteriorated in terms of the observability of celestial bodies. As an example, the numerical value of the measurement for the centre of Rzeszów has been taken. In 2015, this value was 18.70 ± 1.87 mag/arcsec^2, while in 2018, it was equal to 16.73 ± 1.67 mag/arcsec^2. The results obtained were used to analyse the visibility of celestial bodies. Here, particular attention was paid to the analysis of the visibility of comets (also during the outburst), in the context of increasing light pollution of the night sky. Observers in neighboring villages have also experienced a change in the sky quality from Bortle Class V to Class VII, requiring objects to be approximately one magnitude brighter in order to be visible.

Keywords. Light pollution—cometary outburst—visibility of astronomical objects.

1. Introduction

With the development of civilization, the problem of night light pollution is becoming more and more crucial and noticeable in many areas of human activity. One of the first areas of human activity that drew attention to light pollution of the night sky was astronomy. The problem of light pollution of the night sky took on significance at the turn of the 19th and 20th centuries, when electric light was introduced to illuminate cities and routes. This was directly related to the increase in the safety of the region's inhabitants and the prolonging of professional life of people at night. Currently, the most polluted is the night sky with artificial light in the vicinity of large metropolitan cities.

The contamination with the night sky light reduces the contrast between the light of the cosmic bodies and the background of the night sky and therefore it makes observations of astronomical objects of a small brightness extremely difficult or even impossible. Therefore, faint astronomical objects such as comets are difficult to observe even in small cities. What's more, a few (dozen) kilometers away from big cities, the night sky may seem very dark. Even at larger distances from urban centres, where there is only residual light pollution, the visibility of astronomical objects is reduced (Gronkowski *et al.* 2018). It is worth recalling that in such relatively good observational conditions, the human eye notices stars with an apparent magnitude up to +6 mag. However, with a total lack of light pollution, even stars with an apparent magnitude up to +8 mag can be noticeable to the human eye (Curtis 1903).

In recent decades, this problem has become one of the main challenges in observational astronomy. The main reason for the deterioration of the night sky in a given region is the excessive use of artificial lighting. Over the past 30 years, many important works have been published on the subject in which the authors have

Table 1. The Bortle scale is a nine-level numerical scale that measures the brightness of the night sky in a specific location. It defines the observability of celestial bodies in the night sky (Bortle 2001). The following symbol is used in the table: NELM – limiting visibility for the human eye (expressed in mag units). It is worth noting that the Bortle classification refers to the monogram of Spoelstra's brightness (nomogram). In addition, these values form the basis for the predictions of celestial object visibility, including the comets.

Class	Type of sky	Values SQM (mag/arcsec^2)	NELM (mag)
I	Excellent dark-sky site	21.7–22.0	7.6–8.0
II	Typical truly dark site	21.5–21.7	7.1–7.5
III	Rural sky	21.3–21.5	6.6–7.0
IV	Rural/suburban transition	20.4–21.3	6.1–6.5
V	Suburban sky	19.1–20.4	5.6–6.0
VI	Bright suburban sky	18.0–19.1	5.1–5.5
VII	Suburban/urban transition	18.0–19.1	4.6–5.0
VIII	City sky	18.0–19.1	4.1–4.5
IX	Inner-city sky	$\leq$18.0	$\leq$4.0

drawn attention to the growing problem in the context of artificial pollution of the sky (e.g., Garstang 1989; Cinzano *et al.* 2001a, b; Cinzano & Elvidge 2004; Cinzano 2004; Aubé & Kocifaj 2012; Falchi *et al.* 2015; Zamorano *et al.* 2016).

The main purpose of our work is to present the results of measurements of pollution by the artificial light of the night sky in a medium-sized city located in Central Europe. An example of such a city is Rzeszów, which has about 200,000 inhabitants and is located in south-east Poland, near the eastern border of the European Union. Based on the measurements carried out, an analysis of the visibility of celestial bodies in the night sky with a particular consideration of comets was made. In addition, the paper discusses the visibility of a hypothetical comet (X/PC) belonging to the Jupiter family in the night sky during its outburst.

2. Measurement of light pollution in the city of Rzeszów, Poland

2.1 *Measurement methodology – SQM-L*

For determining the night sky brightness, the Bortle IX-scale index (Bortle 2001) is commonly used today. Table 1 presents the visibility ranges related to the observability of celestial bodies depending on the place of observation.

For measuring the degree of the night sky contamination with artificial light, a photometer Sky Quality Meter (SQM-L) was used. It is a hand-held photometer and it could measure the brightness of the night sky in astronomical units of mag/arcsec^2. The photometer has a built-in lens that provides a measurement range limited to an angle of 20°. Thanks to this, we can make accurate measurements of the narrow area of the night sky. To obtain a reliable measurement of the brightness in a given place, it should be repeated several times, because there are differences in brightness between the zenith and other directions in the sky. Note that SQM-L is used by professional as well as amateur astronomers to determine the degree of pollution of the night sky with artificial light with a precision up to 10% (Cinzano 2004). The obtained numerical value is nothing but the apparent brightness of the sky surface in the place where the measurement is made. The result is obtained by summing up the total amount of light entering the photometer through the surface of its field-of-view. Consequently, the obtained measurement indicates the amount of light reaching the photometer from the surface of the observed part of the night sky. To eliminate vibrations of the operator's hand during measurements, the photometer was mounted on a photographic tripod. The examined area of the sky was free from all obstacles, such as trees, buildings, etc.

To get the actual brightness of the sky in a given place, the measurement was repeated ten times on the same day. It is also worth noting that the interval between measurements was about 10 minutes. This was dictated by the fact that the measurement points were distributed all over the street. It should also be emphasized that these measurements were carried out regularly at chosen places. The results of the measurements presented in this paper are average values. The obtained results depend, of course, on the place where the measurements were made, i.e., the type of

Table 2. The brightness of the night sky in Rzeszów at selected points in the city (selected crossroads, roundabouts, avenues, squares, etc.). The measurements were made by means of the Quality Meter (SQM-L). The changes in brightness of the night sky in 2015–2018 are also shown. The measurements of the night sky's brightness according to the SQM-L meter manufacturer's information may be subject to a measurement error of ±10%. The measurements of the night sky brightness are, in general, consistent with the data available on the website (Light pollution map).

Measurement	Values (mag/arcsec^2)	
	2015	2018
Armii Krajowej–Krzyżanowski Roundabout	19.13 ± 1.91	17.58 ± 1.76
Bat. Chłopskich–Langiewicza Crossroads	18.93 ± 1.89	16.79 ± 1.68
Chopin Street	18.74 ± 1.87	17.53 ± 1.75
Ciepliński Avenue	18.68 ± 1.87	17.92 ± 1.79
Dąbrowskiego–Wincentego Pola Crossroads	18.94 ± 1.89	16.68 ± 1.70
Dębicka Street	18.75 ± 1.88	18.05 ± 1.81
Grunwaldzka–Piłsudski Crossroads	18.67 ± 1.87	17.44 ± 1.74
John Paul II Roundabout	18.83 ± 1.88	16.70 ± 1.67
Kopisto–Niepodległości–Rejtana Crossroads	18.97 ± 1.90	16.56 ± 1.65
Kopisto–Podwisłocze Crossroads	18.70 ± 1.87	16.81 ± 1.68
Krakowska Street	18.78 ± 1.88	17.83 ± 1.78
Kuroń Roundabout	18.92 ± 1.89	17.61 ± 1.76
Mazowiecki Bridge	19.18 ± 1.92	18.53 ± 1.85
Pakosław Roundabout	18.74 ± 1.87	16.53 ± 1.65
Piłsudski Avenue	18.77 ± 1.88	16.47 ± 1.64
Pobitno Roundabout	18.98 ± 1.90	16.93 ± 1.69
Powstańców Warszawy Avenue	19.12 ± 1.91	17.32 ± 1.73
Powstańców Warszawy–Dąbrowskiego Crossroads	18.94 ± 1.89	16.57 ± 1.66
Rejtana–Lwowska–Dworaka Crossroads	18.93 ± 1.89	16.90 ± 1.69
Rejtana–Powstańców Warszawy Crossroads	19.15 ± 1.92	16.52 ± 1.66
Rzeszów Market Square	18.70 ± 1.87	16.73 ± 1.67
Śreniawitów Square	18.70 ± 1.87	16.56 ± 1.65
Targowa Street	18.77 ± 1.88	17.78 ± 1.78
Targowa Street (cemetery)	18.75 ± 1.88	16.99 ± 1.70
Witosa-Okulickiego–Krakowska Crossroads	18.86 ± 1.89	16.81 ± 1.68

the night sky (see Table 1). Analysing the numerical values of the night sky brightness, one can notice a certain regularity. If the sky is darker, the photometer (SQM-L) records a larger numerical value of the sky brightness. Similarly, when the sky is brighter, for example in the city centre, the device displays a smaller measurement value. The presented classification of the measurements is consistent with the classical scale of the astronomical objects' brightness, i.e., the scale of brightness magnitude according to the Pogson formula.

2.2 *The brightness of the night sky over Rzeszów – Results*

The measurements of the brightness of the night sky were carried out in Rzeszów in 2015 and 2018. The obtained results of measurements show how the types of night sky changed over the centre of Rzeszów. The results were grouped for the city centre (Table 2) and the surrounding area (Table 3). When interpreting the results, one can conclude that unfortunately, the quality of the sky in terms of astronomical objects' visibility in Rzeszów significantly deteriorated during these three years (2015–2018). The main reason for this is the dynamic development of the region, in particular, of the neighbouring villages. This problem is particularly important in the context of conducting astronomical observations comets, but not only. To illustrate this situation from the observational astronomy point of view, we present pictures of afterglow in Rzeszów (Fig. 1). It is easy to see how the night sky is polluted with artificial light, which makes it difficult or even impossible to

Table 3. The same as in Table 2, but the measurements were carried out in the vicinity of Rzeszów. The average distance (in kilometers) between given location and the city centre are also displayed.

	Values (mag/arcsec^2)	
Measurement	2015	2018
A4 highway ($d = 11.9$ km)	20.30 ± 2.03	18.52 ± 1.85
Biała ($d = 6.7$ km)	20.01 ± 2.00	18.84 ± 1.88
Boguchwała ($d = 7.9$ km)	19.68 ± 1.97	18.64 ± 1.86
Bzianka ($d = 9.6$ km)	20.39 ± 2.04	18.26 ± 1.83
Kielnarowa ($d = 12.7$ km)	20.85 ± 2.09	18.90 ± 1.89
Krasne ($d = 7.6$ km)	20.05 ± 2.00	17.57 ± 1.76
Malawa ($d = 7.7$ km)	20.49 ± 2.05	19.54 ± 1.95
Matysówka ($d = 8.4$ km)	20.96 ± 2.10	20.22 ± 2.02
Miłocin ($d = 4.4$ km)	19.70 ± 1.97	18.81 ± 1.88
Przybyszówka ($d = 5.7$ km)	19.60 ± 1.96	17.67 ± 1.77
Rogoźnica ($d = 10.8$ km)	20.40 ± 2.04	18.93 ± 1.89
Słocina ($d = 5.9$ km)	19.51 ± 1.95	19.92 ± 1.99
Trzebownisko ($d = 13.2$ km)	19.95 ± 2.00	18.50 ± 1.85
Tyczyn ($d = 10.1$ km)	20.52 ± 2.05	18.93 ± 1.89
Zaczernie ($d = 7.6$ km)	20.18 ± 2.02	18.43 ± 1.84

Figure 1. The pollution of the sky by artificial light over Rzeszów. The photo was taken from the Matysówka hill.

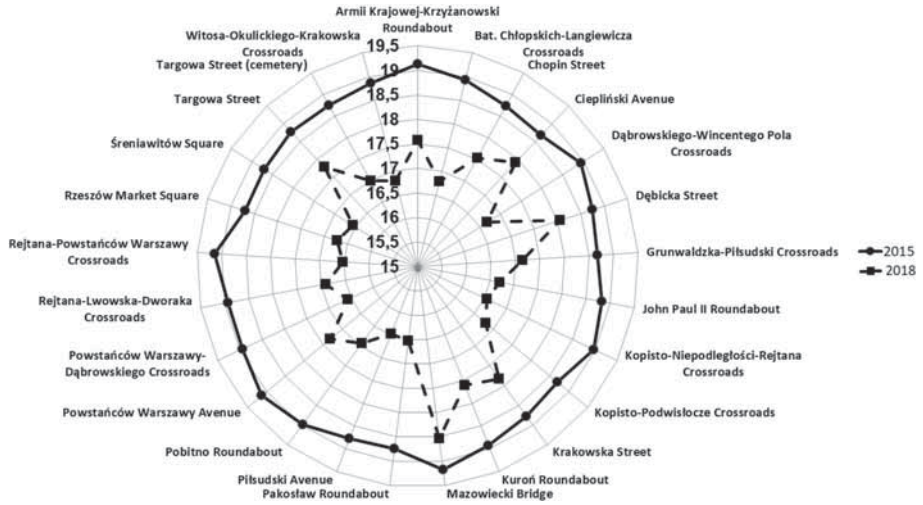

Figure 2. Distribution of changes in the surface brightness of the night sky (expressed in mag/arcsec^2 units) in Rzeszów in the context of artificial light pollution in the years 2015–2018.

Figure 3. The same as in Fig. 2, but here it refers to selected neighbouring villages near Rzeszów.

observe small celestial bodies even in the neighbouring villages. The distribution of changes in the brightness of the night sky in Rzeszów in 2015 and 2018 is shown in Figures 2–3.

The obtained results demonstrate how the state of the night sky has changed in the city centre and surrounding villages in 2015–2018. It is easy to notice that the state of the night sky in Rzeszów in 2018 deteriorated in comparison to 2015: the brightness of the night sky in the city centre increased, and thus the visibility of faint astronomical objects deteriorated.

With respect to the Bortle classification, a jump in brightness surface of the sky by two types of night sky (VII to IX, see Table 2) was recorded. In the case of the neighbouring villages, this increase also changed, on average, by two types of night sky (from V to VII, see Table 3), and Figure 4. One can notice a significant increase in the pollution of the night sky by artificial light in Rzeszów in such a short period of time. It is worth noticing that the results obtained by means of the SQM-L meterand presented in Tables 2–3 are consistent with the satellite measurements displayed in the form of maps in Fig. 4.

3. Real visibility of selected comets in the night sky in Rzeszów

The night sky polluted by the artificial light makes the observation of comets very difficult or even impossible because of their poor initial brightness. Sometimes however, comets exhibit a very large, sudden and unexpected increase in brightness, which we call cometary outbursts. In the maximum of the outburst, the

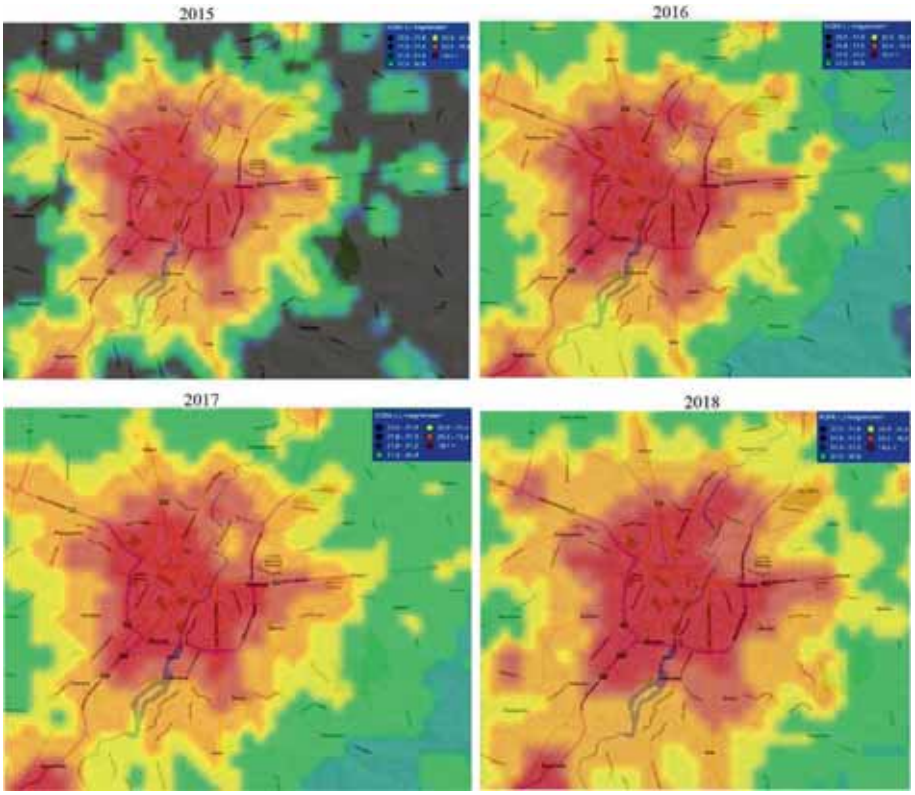

Figure 4. Distribution of surface brightness of the night sky in Rzeszów in the years 2015–2018 in the context of artificial light pollution (Source: Light pollution map).

brightness of the comet is usually a few magnitudes larger in comparison to the phase before the outburst. It should be clarified that the outburst of cometary brightness can not be identified with a physical explosion, such as a bomb explosion. This is only a huge brightening of the comet associated with the emission of matter from its nucleus. According to the astronomers who studied this phenomenon, their direct cause is related to the ejection of an outer surface of the comet's nucleus (Gronkowski & Wesołowski 2015 and literature therein). The rapid changes in the brightness of the comet is so interesting that many astronomers around the world are still looking for their causes (Richter 1954; Hughes 1990, 1991; Cabot 1996; Enzian 1997; Groussin *et al.* 2004; Trigo-Rodriguez 2008a, b, 2010; Ivanova 2011; Gronkowski & Wesołowski 2012; Wesołowski & Gronkowski 2018a).

In scientific literature related to this searching, a number of more or less plausible mechanisms have been proposed. The analysis of these different mechanisms is not the purpose of this paper, so readers who are interested in the topic may familiarize themselves with the papers devoted to the cometary outbursts (see, for e.g., Hughes 1990; Gronkowski & Wesołowski 2016). As it has already been mentioned that at the time of the outburst, the glow of a comet rapidly increases. As a result, a comet under favourable circumstances becomes an object visible in the night sky, even in the centre of large cities. An example of this is the famous comet 17P/Holmes, which in November 2007 underwent a very large outburst of brightness. This outburst was the most spectacular in the entire history of astronomical observations because its amplitude in the BVRI photometric bands was around −14 magnitudes (Montalto 2008)! It is worth recalling that Ścieżor (2013) used the observation of the comet's brightness to determine the degree of pollution by the artificial light of the night sky.

His method is based on the measurements of the surface brightness of the faintest diffusive astronomical objects that are visible in the night sky. Such diffusive objects selected for observation must be characterized by flat brightness distributions without any highlighted maximum. Therefore, generally such astronomical objects such as galaxies, star clusters or nebulae are not suitable for this purpose, while a number of comets meet this criterion. For an observer, the majority of comets are fuzzy objects whose surface brightness steadily decreases from the inside outwards, until it merges with the background of the sky. That is why determination of the night sky surface brightness is called the cometary method. In order to determine

Table 4. Actual visibility by the naked eye of different comets in the night sky according to Bortle classification. The '+' sign means that the comet is visible; the '–' sign means that the comet is invisible. In the calulations, the data releted to the quality of night sky (Table 1) were taken into account. It was assumed that the parameter $m(t_{\max})$ means the actual brightness of the comet which can be associated with its outburst (Fernández 1999; Tancredi 2000 and literature therein).

	Type of sky								
Example – the comet	I	II	III	IV	V	VI	VII	VIII	IX
C/2006 P1 – $m(t_{\max}) \approx -5.^{\mathrm{m}}5$	+	+	+	+	+	+	+	+	+
C/2011 W3 – $m(t_{\max}) \approx -4.^{\mathrm{m}}0$	+	+	+	+	+	+	+	+	+
C/1995 O1 – $m(t_{\max}) \approx -1.^{\mathrm{m}}0$	+	+	+	+	+	+	+	+	+
C/2002 V1 – $m(t_{\max}) \approx 2.^{\mathrm{m}}0$	+	+	+	+	+	+	+	+	+
17P/Holmes – $m(t_{\max}) \approx 2.^{\mathrm{m}}5$	+	+	+	+	+	+	+	+	+
C/2004 F4 – $m(t_{\max}) \approx 3.^{\mathrm{m}}0$	+	+	+	+	+	+	+	+	+
C/2001 Q4 – $m(t_{\max}) \approx 3.^{\mathrm{m}}5$	+	+	+	+	+	+	+	+	+
C/2006 M4 – $m(t_{\max}) \approx 4.^{\mathrm{m}}0$	+	+	+	+	+	+	+	+	+
C/2001 A2 – $m(t_{\max}) \approx 4.^{\mathrm{m}}5$	+	+	+	+	+	+	+	+	-
103P/Hartley – $m(t_{\max}) \approx 5.^{\mathrm{m}}0$	+	+	+	+	+	+	+	-	-
C/2009 R1 – $m(t_{\max}) \approx 5.^{\mathrm{m}}5$	+	+	+	+	+	+	-	-	-
8P/Tuttle – $m(t_{\max}) \approx 6.^{\mathrm{m}}0$	+	+	+	+	+	-	-	-	-
29P/SW – $m(t_{\max}) \approx 13.^{\mathrm{m}}0$	-	-	-	-	-	-	-	-	-
1P/Halley – $m(t_{\max}) \approx 19.^{\mathrm{m}}0$	-	-	-	-	-	-	-	-	-

the degree of comet condensation, the DC (degree of condensation) was introduced; it describes the amount of blur of the comet against the background of the sky. This value determines the gradient between the centre of the comet envelope and its bank. A comet with DC = 9 looks like a star, while a comet with DC = 0 has a flat distribution of brightness, and its surface brightness is practically equal to that of the surrounding sky background. A comet with DC = 5 has a clear, brighter nucleus and an envelope blurred by the background of the sky. This means that for the most vulnerable comets that can be visible in the telescope (or binoculars or even by the naked eye) with very low DC (from 0 to 2), their surface brightness can serve as an approximate value of the sky surface brightness – more precisely, it defines the lower limit of the sky surface brightness (Gronkowski *et al.* 2018).

As an example, in Table 4, some chosen comets are presented with the visibility in a given type of sky. We include two types of comets whose brightness changes due to intense sublimation (e.g. C/1995 O1) or those that outburst (e.g. 17P/Holmes).

4. The outburst of the comet and its visibility in the night sky: Numerical simulation

As mentioned above, the comets in a non-outburst state are generally the objects of low brightness and therefore, they are difficult to be observed in the night sky. However, during the outburst their brightness may increase by a dozen of magnitudes. Then they can even become the objects of dominant brightness in the night sky. The authors of various hypotheses trying to explain the phenomenon of a comet outburst believe that the direct cause is the ejection of the surface layer of the nucleus. It will be very instructive to examine how comet visibility in the night sky depends upon the amount of mass ejected from the nucleus. This issue has already been studied by Wesołowski & Gronkowski (2018a, b). Therefore now only the basic assumptions and facts related to this issue is recalled. The rejection of the matter layer from the comet's nucleus leads to (a) increase in the amount of matter that reflects sunlight in the atmosphere comets, and (b) an explosion exposes the deeper nucleus layers that are richer in volatile substances. All of these quickly increase the glow of the comet and ultimately lead to an outburst of its brightness. In other words, we suppose that the direct cause of the cometary outbursts are the ejection of the outer surface layer from the part of the nucleus and the increase in the rate of cometary matter sublimation. To simplify the calculations, we assumed the ejected cometary material having the form of a cloud of ice-dust grains having spherical shape. The brightness of the comet depends essentially on the rate of sublimation from the surface of its nucleus. On the other hand, the surface temperature of the nucleus determines the rate of sublimation

Table 5. Values of the physical cometary parameters for object X/PC used in the numerical calculations and simulations. They are the same as in Richardson (2007), Reach (2010), Kossacki & Szutowicz (2013), Gronkowski & Wesołowski (2015, 2017) and literature therein.

Parameter	Values
Albedo (–)	$A_{\mathrm{N}} = 0.04$
Semi-major axis of the cometary orbit (au)	$a = 3.00$
Eccentricity of the cometary orbit (–)	$e = 0.666(6)$
Orbital inclination of the cometary orbit (°)	$i = 0$
Perihelion of the cometary orbit (au)	$q = 1.00$
Aphelion of the cometary orbit (au)	$Q = 5.00$
Tisserand parameter for the comet considered in this paper (–)	$T_{\mathrm{J}} = 2.87$
Density of the comet nucleus (kg · m^{-3})	$\rho_{\mathrm{N}} = 400$
Radius of the comet nucleus (m)	$R_{\mathrm{N}} = 2000$
Hertz factor (–)	$h(\psi) = 0.001$
Porosity (–)	$\psi = 0.75$
Dust–gas mass ratio (–)	$\kappa = 1$
Radius of the cometary head during the outburst (m)	$R'_{\mathrm{h}} = 3 \cdot 10^8$
Radius of the cometary head in the gentle sublimation (m)	$R_{\mathrm{h}} = 1 \cdot 10^8$
Minimum radius of cometary grains (m)	$a_{\min} = 10^{-7}$
Maximum radius of cometary grains (m)	$a_{\max} = 10^{-2}$
Mean value of wavelength of solar radiation (m)	$\lambda = 0.5015 \cdot 10^{-6}$

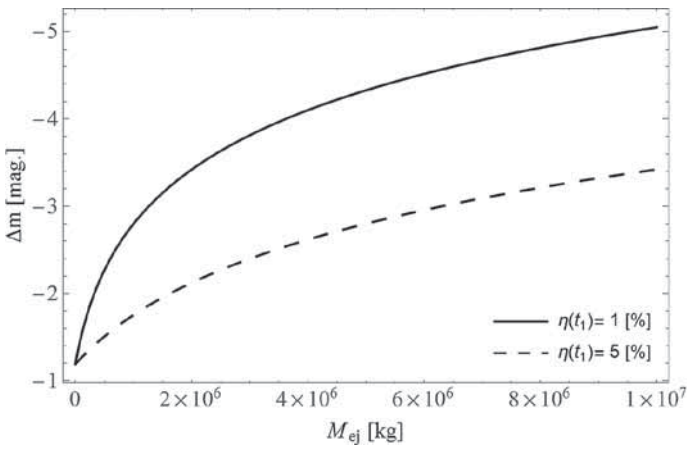

Figure 5. Jump Δm in the cometary brightness as a function of the ejected mass M_{ej} from the nucleus of the comet X/PC for different values of the parameter $\eta(t_1)$. It assumed that the comet is at perihelion of its orbit $d = 1.00$ au.

from the comet. Therefore, first we have to solve the energy balance equation for the comet nucleus relative to its surface temperature T. The equation is as follows:

$$\frac{S_{\odot}(1 - A_{\mathrm{N}})\cos\varphi}{d^2} = \epsilon\,\sigma\,T^4 + \eta\frac{\dot{Z}\,L(T)}{N_{\mathrm{A}}} + h(\psi)\,K(T)\,\nabla T. \quad (1)$$

In Equation (1), the left-hand side denotes solar radiation energy absorbed by the nucleus, and the right-hand side is a sum of three terms: energy re-radiated by the nucleus, the energy used for the sublimation of cometary ice and the heat conducted into the interior of the comet nucleus. We accept here the following notations: $S_{\odot}$ is the solar constant at heliocentric distance $d = 1$ au, A_{N} is the albedo of the cometary nucleus, φ is the angle between the normal to the surface of the nucleus and the direction to the Sun, d is the heliocentric distance of the comet, ϵ is the infrared emissivity of the nucleus, σ is the Stefan–Boltzmann constant, η is the percentage of the active sublimation

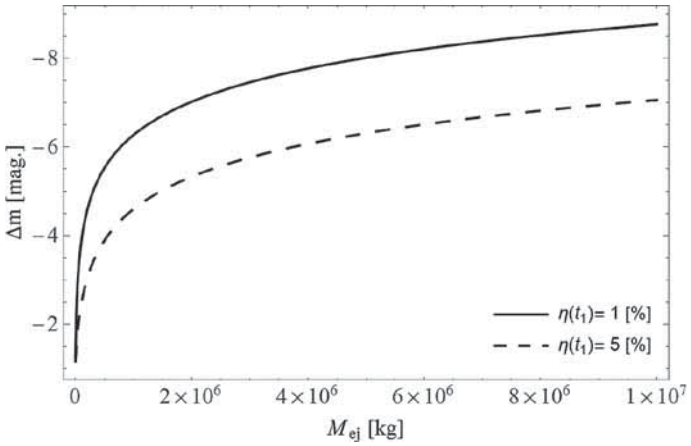

Figure 6. Same as in Fig. 5, but it is assumed that the comet is at an average distance of $d = 3.00$ au.

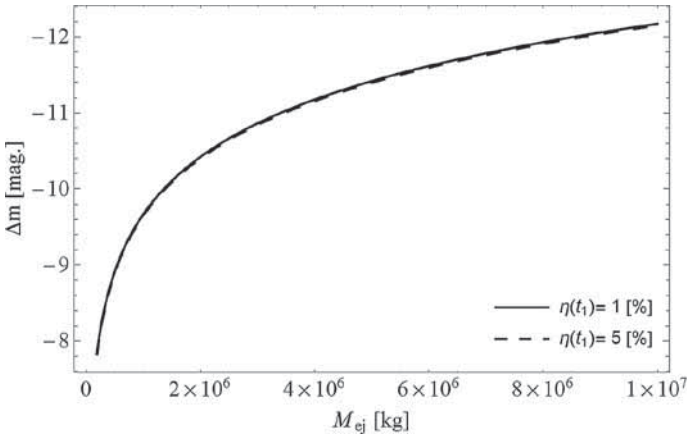

Figure 7. Same as in Fig. 5, but it is assumed that the comet is at the aphelion $d = 5.00$ au.

Table 6. Jump Δm in the cometary brightness as a function of the heliocentric distance d of the X/PC and the parameter $\eta(t_1)$. We assume that the $M_{\rm ej} = 10^7$ kg.

	Δm (mag.)	
	$\eta(t_1)(\%)$	
d (au)	1	5
1.00	–5.05	–3.42
3.00	–8.76	–7.06
5.00	–12.17	–12.15

surface of the comet nucleus, $\dot{Z}$ is the rate of sublimation from the nucleus surface, $L(T)$ is the latent heat of cometary ice sublimation, $N_{\rm A}$ is the Avogadro number and $K(T)$ is the average heat conductivity of a cometary nucleus. We note that the heat conductivity $K(T)$ is corrected by a Hertz factor $h(\psi)$ depending on the porosity ψ, because porosity leads to the reduction of the contact surface between cometary grains (Davidsson & Skorov 2002). Knowing the surface temperature of the comet's nucleus, we can easily determine the amplitude of its brightness jump Δm based on the Pogson formula (for more information, see for e.g., Gronkowski 2007, 2009; Gronkowski & Wesołowski 2015 and references therein):

$$\begin{aligned}\Delta m &= m(t_2) - m(t_1) \\ &= -2.5 \log \frac{C_{\rm s}(n) + C_{\rm s}(t_2) + C_{\rm s}(M_{\rm ej})}{C_{\rm s}(n) + C_{\rm s}(t_1)},\end{aligned} \tag{2}$$

In Equation (2), $m(t_2)$ and $m(t_1)$ indicate the comet's brightness in the calm phase and in the outburst phase respectively, $C_{\rm s}(n)$ stands for the scattering cross-section of the bare comet's nucleus ($C_{\rm s}(n) = A_{\rm N}\pi R_{\rm N}^2$), where $R_{\rm N}$ is the radius of the nucleus. The $C_{\rm s}(t_1)$ and $C_{\rm s}(t_2)$ denote the total scattering cross-sections of the cometary water–ice dust particles that were raised by sublimation and remain in

Table 7. The naked-eye visibility of X/PC in the night sky over Rzeszów as a function of assumed cometary luminosity $m(t_1)$. In the first column, there are classes of the night sky according to Bortle classification. It is assumed that X/PC is in the heliocentric distance $d = 1.00$ au and the jump in its brightness is $\Delta m = -5.05$ magnitude (according to Table 6). The calculations were done with the parameter $\eta(t_1) = 1\%$. The following signs were adopted: '+' denotes that the comet is visible and '–' denotes that the comet is invisible.

	$m(t_1)$ (mag)					
Type of sky	8	10	12	14	16	18
1	+	+	+	–	–	–
2	+	+	+	–	–	–
3	+	+	+	–	–	–
4	+	+	-	–	–	–
5	+	+	–	–	–	–
6	+	+	–	–	–	–
7	+	+	–	–	–	–
8	+	–	–	–	–	–
9	+	–	–	–	–	–

Table 8. Same as in Table 7, but it is assumed that comet X/PC is in the heliocentric distance $d = 3.00$ au and the parameter $\Delta m = -8.74$ magnitude.

	$m(t_1)$ (mag)					
Type of sky	8	10	12	14	16	18
1	+	+	+	+	+	–
2	+	+	+	+	+	–
3	+	+	+	+	–	–
4	+	+	+	+	–	–
5	+	+	+	+	–	–
6	+	+	+	+	–	–
7	+	+	+	–	–	–
8	+	+	+	–	–	–
9	+	+	+	–	–	–

coma in the normal inactive phase and in the active outburst phase, respectively. These scattering cross-sections depend on the total number of cometary particles remaining in the head of the comet during these two phases: $N_{\mathrm{gr}}(t_1)$ and $N_{\mathrm{gr}}(t_2)$, respectively. Here $f(a)$ stands for their size distribution function. Note that the parameter $C_{\mathrm{s}}(M_{\mathrm{ej}})$ occurring in Equation (2) denotes the total scattering cross-section of the cometary debris created after destruction of the surface nucleus layers. The global scattering

Table 9. Same as in Table 7, but it is assumed that comet X/PC is in the heliocentric distance $d = 5.00$ au and the parameter $\Delta m = -12.17$ magnitude.

	$m(t_1)$ (mag)					
Type of sky	8	10	12	14	16	18
1	+	+	+	+	+	+
2	+	+	+	+	+	+
3	+	+	+	+	+	+
4	+	+	+	+	+	+
5	+	+	+	+	+	+
6	+	+	+	+	+	–
7	+	+	+	+	+	–
8	+	+	+	+	+	–
9	+	+	+	+	+	–

cross-section of all cometary particles (grains) is given by the following expression:

$$C_{\mathrm{sca}}(t_i) = \pi N_{\mathrm{gr}}(t_i) \int_{\mathrm{a_{min}}}^{\mathrm{a_{max}}} Q(\lambda, a, m) a^2 f(a) da, \quad (3)$$

Here $i = 1$ or 2, and we accept the following notation: λ is the wavelength of the electromagnetic solar radiation, a is the radius of a cometary grain and m is the complex effective index of the grain material, while $Q(\lambda, a, m) = Q$ are the scattering efficiencies of the cometary grains. These scattering efficiencies occurring in Equation (3) were calculated by means of Mie theory (see, for e.g., Bohren & Huffman 1983). Eventually, based on the last two equations, one can derive the final formula which describes the amplitude of the comet's glow during its outburst (Wesołowski & Gronkowski 2018a):

$$\Delta m = -2.5 \log \left(\frac{1 + \frac{\kappa \eta(t_2) \dot{Z} R'_{\mathrm{h}} m_g}{v_{\mathrm{g}} \cdot A_{\mathrm{N}}} \cdot A + \frac{M_{\mathrm{ej}}}{4 C_{\mathrm{s}}(n)} \cdot A}{1 + \frac{\kappa \eta(t_1) \dot{Z} R_{\mathrm{h}} m_g}{v_{\mathrm{g}} \cdot A_{\mathrm{N}}} \cdot A} \right), \quad (4)$$

where

$$A = \frac{3 \cdot \int_{\mathrm{a_{min}}}^{\mathrm{a_{max}}} Q a^2 f(a) da}{\rho_{\mathrm{gr}} \cdot \int_{\mathrm{a_{min}}}^{\mathrm{a_{max}}} a^3 f(a) da}. \quad (4a)$$

In the above expressions, we use the following notations: κ is the dust–gas mass ratio ($\kappa = 1$), R'_{h} stands for the radius of the cometary head during the outburst, R_{h} stands for the radius of the cometary head in the gentle sublimation phase, m_{g} is the mass of grains, ρ_{gr} denotes

Table 10. The visibility of the planets. The maximum brightness of the planets was taken into account in the calculations taken from the visibility of the planets.

	Type of sky								
Planets of the solar system	I	II	III	IV	V	VI	VII	VIII	IX
Mercury – $m(t_{\max}) = -2^{\mathrm{m}}.45$	+	+	+	+	+	+	+	+	+
Venus – $m(t_{\max}) = -4.^{\mathrm{m}}89$	+	+	+	+	+	+	+	+	+
Mars – $m(t_{\max}) = -2.^{\mathrm{m}}91$	+	+	+	+	+	+	+	+	+
Jupiter – $m(t_{\max}) = -2.^{\mathrm{m}}94$	+	+	+	+	+	+	+	+	+
Saturn – $m(t_{\max}) = -0.^{\mathrm{m}}49$	+	+	+	+	+	+	+	+	+
Uranus – $m(t_{\max}) = 5.^{\mathrm{m}}32$	+	+	+	+	+	+	–	–	–
Neptune – $m(t_{\max}) = 7.^{\mathrm{m}}78$	+	–	–	–	–	–	–	–	–

Table 11. The visibility of planets. The minimum brightness of the planets was taken into account in the calculations taken from the visibility of the planets.

	Type of sky								
Planets of the solar system	I	II	III	IV	V	VI	VII	VIII	IX
Mercury – $m(t_{\min}) = 5^{\mathrm{m}}.73$	+	+	+	+	+	–	–	–	–
Venus – $m(t_{\min}) = -3.^{\mathrm{m}}82$	+	+	+	+	+	+	+	+	+
Mars – $m(t_{\min}) = 1.^{\mathrm{m}}84$	+	+	+	+	+	+	+	+	+
Jupiter – $m(t_{\min}) = -1.^{\mathrm{m}}61$	+	+	+	+	+	+	+	+	+
Saturn – $m(t_{\min}) = 1.^{\mathrm{m}}47$	+	+	+	+	+	+	+	+	+
Uranus – $m(t_{\min}) = 5.^{\mathrm{m}}95$	+	+	+	+	+	-	–	–	–
Neptune – $m(t_{\min}) = 8.^{\mathrm{m}}02$	–	–	–	–	–	–	–	–	–

Table 12. The visibility of dwarf planets.

	Type of sky								
Examples of dwarf planets	I	II	III	IV	V	VI	VII	VIII	IX
Ceres – $m = 6^{\mathrm{m}}.7$	+	+	+	–	–	–	–	–	–
Pluto – $m = 15.^{\mathrm{m}}0$	–	–	–	–	–	–	–	–	–
Makemake – $m = 17.^{\mathrm{m}}0$	–	–	–	–	–	–	–	–	–
Haumea – $m = 17.^{\mathrm{m}}3$	–	–	–	–	–	–	–	–	–
Eris – $m = 18.^{\mathrm{m}}7$	–	–	–	–	–	–	–	–	–

the density of the grains and v_{g} stands for the mean radial velocity of the gas molecules; $\eta(t_1)$ and $\eta(t_2)$ are the percentage of the active sublimation surface of the comet's nucleus in the calm phase and the active outburst phase, respectively. Other symbols have their usual meaning. The calculations of the amplitude jump in the brightness during the cometary outbursts were made for the hypothetical comet X/PC that belongs to the Jupiter family comets (hereafter JFCs).

4.1 *Results of numerical calculations*

The numerical values of physical parameters which were used in the calculations are presented in Table 5. The results of numerical simulations are presented in the form of graphs (Figs. 5–7 and Tables 6–9). The calculations were carried out for three model heliocentric distances ($d = 1$ au, $d = 3$ au, $d = 5$ au). In addition, it is assumed that the activity of the comet

Table 13. The visibility of the brightest stars from the constellation, the Ursa Major (Great Bear), taken from list of stars in Ursa Major.

	Type of sky								
Examples of stars	I	II	III	IV	V	VI	VII	VIII	IX
ε UMa – $m = 1^{\mathrm{m}}.76$	+	+	+	+	+	+	+	+	+
α UMa – $m = 1^{\mathrm{m}}.81$	+	+	+	+	+	+	+	+	+
η UMa – $m = 1^{\mathrm{m}}.85$	+	+	+	+	+	+	+	+	+
ξ UMa – $m = 2^{\mathrm{m}}.23$	+	+	+	+	+	+	+	+	+
β UMa – $m = 2^{\mathrm{m}}.34$	+	+	+	+	+	+	+	+	+
γ UMa – $m = 2^{\mathrm{m}}.41$	+	+	+	+	+	+	+	+	+
ψ UMa – $m = 3^{\mathrm{m}}.00$	+	+	+	+	+	+	+	+	+
μ UMa – $m = 3^{\mathrm{m}}.06$	+	+	+	+	+	+	+	+	+

Table 14. The visibility of the brightest stars from the Cassiopeia constellation, taken from list of stars in Cassiopeia.

	Type of sky								
Examples of stars	I	II	III	IV	V	VI	VII	VIII	IX
γ Cas – $m = 2^{\mathrm{m}}.15$	+	+	+	+	+	+	+	+	+
α Cas – $m = 2^{\mathrm{m}}.24$	+	+	+	+	+	+	+	+	+
β Cas – $m = 2^{\mathrm{m}}.28$	+	+	+	+	+	+	+	+	+
δ Cas – $m = 2^{\mathrm{m}}.68$	+	+	+	+	+	+	+	+	+
ε Cas – $m = 3^{\mathrm{m}}.35$	+	+	+	+	+	+	+	+	+
η Cas – $m = 3^{\mathrm{m}}.46$	+	+	+	+	+	+	+	+	+
ζ Cas – $m = 3^{\mathrm{m}}.69$	+	+	+	+	+	+	+	+	+
50 Cas – $m = 3^{\mathrm{m}}.95$	+	+	+	+	+	+	+	+	+

Table 15. The visibility of the brightest stars from the Draco (Dragon) constellation, taken from list of stars in Draco.

	Type of sky								
Examples of stars	I	II	III	IV	V	VI	VII	VIII	IX
γ Dra – $m = 2^{\mathrm{m}}.24$	+	+	+	+	+	+	+	+	+
η Dra – $m = 2^{\mathrm{m}}.73$	+	+	+	+	+	+	+	+	+
β Dra – $m = 2^{\mathrm{m}}.79$	+	+	+	+	+	+	+	+	+
δ Dra – $m = 3^{\mathrm{m}}.07$	+	+	+	+	+	+	+	+	+
ζ Dra – $m = 3^{\mathrm{m}}.17$	+	+	+	+	+	+	+	+	+
| Dra – $m = 3^{\mathrm{m}}.29$	+	+	+	+	+	+	+	+	+
χ Dra – $m = 3^{\mathrm{m}}.55$	+	+	+	+	+	+	+	+	+
Thuban Dra – $m = 3^{\mathrm{m}}.67$	+	+	+	+	+	+	+	+	+

was controlled by sublimating water ice along the entire comet's orbit.

5. Visibility of selected astronomical objects on the night sky over Rzeszów

In this section, we present selected values of celestial bodies visibility (planets, dwarf planets, selected comets and selected stars in the constellations: the Ursa Major, the Cassiopeia, the Draco, the Cepheus, the Ursa Minor and the Camelopardalis. For this purpose, we re-use the 9-grade Bortle classification (Table 1). By calculating the visibility of a given star in the night sky, its brightness was taken from the Bright Star Catalogue. It is worth noting that this catalogue contains a list of almost all stars whose brightness is greater than

Table 16. The visibility of the brightest stars from the Cepheus constellation, taken from list of stars in Cepheus.

	Type of sky								
Examples of stars	I	II	III	IV	V	VI	VII	VIII	IX
α Cep $- m = 2^{\mathrm{m}}.45$	+	+	+	+	+	+	+	+	+
γ Cep $- m = 3^{\mathrm{m}}.21$	+	+	+	+	+	+	+	+	+
β Cep $- m = 3^{\mathrm{m}}.23$	+	+	+	+	+	+	+	+	+
ζ Cep $- m = 3^{\mathrm{m}}.39$	+	+	+	+	+	+	+	+	+
η Cep $- m = 3^{\mathrm{m}}.41$	+	+	+	+	+	+	+	+	+
| Cep $- m = 3^{\mathrm{m}}.50$	+	+	+	+	+	+	+	+	+
δ Cep $- m = 4^{\mathrm{m}}.07$	+	+	+	+	+	+	+	+	−
$\varepsilon Cep - m = 4^{\mathrm{m}}.18$	+	+	+	+	+	+	+	+	−

Table 17. The visibility of the brightest stars from the constellation, the Ursa Minor (Little Bear), taken from list of stars in Ursa Minor.

	Type of sky								
Examples of stars	I	II	III	IV	V	VI	VII	VIII	IX
α UMi $- m = 1^{\mathrm{m}}.97$	+	+	+	+	+	+	+	+	+
β UMi $- m = 2^{\mathrm{m}}.07$	+	+	+	+	+	+	+	+	+
γ UMi $- m = 3^{\mathrm{m}}.04$	+	+	+	+	+	+	+	+	+
$\varepsilon UMi - m = 4^{\mathrm{m}}.21$	+	+	+	+	+	+	+	+	−
5 UMi $- m = 4^{\mathrm{m}}.25$	+	+	+	+	+	+	+	+	−
ζ UMi $- m = 4^{\mathrm{m}}.29$	+	+	+	+	+	+	+	+	−
δ UMi $- m = 4^{\mathrm{m}}.35$	+	+	+	+	+	+	+	+	−
RR UMi $- m = 4^{\mathrm{m}}.63$	+	+	+	+	+	+	+	−	−

Table 18. The visibility of the brightest stars from the Camelopardalis (Giraffe) constellation, taken from the list of stars in Camelopardalis.

	Type of sky								
Examples of stars	I	II	III	IV	V	VI	VII	VIII	IX
β Cam $- m = 4^{\mathrm{m}}.03$	+	+	+	+	+	+	+	+	−
CS Cam $- m = 4^{\mathrm{m}}.21$	+	+	+	+	+	+	+	+	−
α Cam $- m = 4^{\mathrm{m}}.26$	+	+	+	+	+	+	+	+	−
BE Cam $- m = 4^{\mathrm{m}}.39$	+	+	+	+	+	+	+	+	−
7 Cam $- m = 4^{\mathrm{m}}.43$	+	+	+	+	+	+	+	+	−
CE Cam $- m = 4^{\mathrm{m}}.55$	+	+	+	+	+	+	+	−	−
M Cam $- m = 4^{\mathrm{m}}.55$	+	+	+	+	+	+	+	−	−
γ Cam $- m = 4^{\mathrm{m}}.59$	+	+	+	+	+	+	+	−	−

$+6^{\mathrm{m}}.5$. In order to accurately determine the visibility of a given star in the night sky, advanced computational methods should be applied, which use, among others, professional satellite images (Cinzano *et al.* 2001a). The visibility calculations for these objects are presented in the Tables 10–18.

6. Conclusion

The increasing brightness of the night sky influences negatively on the observation of comets even during their violent outbursts. In Table 4, the data related to the selected comets are tallied; data includes their maximum brightness at their outbursts and their visibility on a given type of night sky. For the comet to be visible to the naked eye in the night sky in the city centre, the jump of its brightness must be considerable.

In the context of planning and carrying out astronomical observations in the vicinity of large cities, the so-called island range light should be considered. From the analysis of measurements done in the case of Rzeszów, this range is around 20 km from the city centre, on average. In the case of the neighbouring villages, this range is estimated at 3–7 km. When planning observations of planets or stars, one should choose areas that are relatively free from light pollution, however, this is not so easy to do at our times. According to Polish astronomers, relatively good conditions for carrying out observations can be found in the mountain ranges of the Carpathian Mountains. The results presented in the work are related mainly to the visibility of comets (also during their outburst) in the night sky. The results of calculations are presented in Tables 6–9 and Figs. 5–7. Due to the analysis of the hypothetical comet (X/PC) during its outburst, we are able to estimate the influence of night sky quality on the visibility of these objects.

In addition, the paper also presents visibility in the night sky of the following celestial bodies: planets (Tables 10–11), dwarf planets (Table 12), and six circumpolar constellations visible in Poland (Tables 13–18). The following conclusions can be drawn from the results presented in these tables:

- in the case of planets, most of them are visible in Rzeszów on every type of sky, regardless of the maximum or minimum of their brightness,
- the first exception to this rule is Uranus and Neptune, which are visible only on the dark type of the sky, due to the relative low brightness in relation to other planets,
- the second exception is Mercury. In this case, it results from the large differences in brightness during the periods of their maximum and minimum brightness (from 5.73 mag to –2.45 mag).

The next example of astronomical objects are stars, which are, in particular, constellations. The following six constellations around the polar area were taken into account: Ursa Maior, Cassiopeia, Dragon, Cepheus, Ursa Minor and Camelopardis. In the case of individual constellations, the visibility of 8 brightest stars from each constellation was examined, using Bortle classification.

The results of measurements presented in the paper clearly demonstrate that the surface brightness of the night sky in Rzeszów and its vicinity has greatly increased during the considered period of time. No doubt, the sky light pollution has a huge impact on the visibility of astronomical objects in the night sky in the context of conducting professional and amateur astronomical observations.

Acknowledgements

The author would like to express his gratitude to the anonymous reviewer for very helpful comments that have considerably improved the quality of the manuscript. This paper was written due to the support the author received from the Centre for Innovation and Transfer of Natural Sciences and Engineering Knowledge at the University of Rzeszów.

References

Aubé M., Kocifaj M. 2012, Using two light-pollution models to investigate artificial sky radiances at Canary Islands observatories, MNRAS, 422, 819 (2012)

Bohren C. F., Huffman D. 1983, Absorption and Scattering of Light by Small Particles, Wiley, New York

Bortle J. E. 2001, Introducing the Bortle Dark-Sky Scale, Sky and Telescope, vol. 101, p. 126

Cabot H. *et al.* 1996, Complementary studies on the unexpected activity of comet Schwassmann–Wachmann 1, Planet & Space Sci., 44, 1015

Cinzano P., Falchi F., Elvidge C. D. 2001a, Naked-eye star visibility and limiting magnitude mapped from DMSP-OLS satellite data, MNRAS, 323, 34

Cinzano P., Falchi F., Elvidge C. D. 2001b, The first World Atlas of the artificial night sky brightness, MNRAS, 328, 689

Cinzano P., Elvidge C. D. 2004, Night sky brightness at sites from DMSP-OLS satellite measurements, MNRAS, 353, 1107

Cinzano P. 2004, A portable spectrophotometer for light pollution measurements, Memorie della Società Astronomica Italiana Suppl., 5, 395

Curtis H. D. 1903, On the limits of unaided vision, Lick Observatory Bull., 2, 67

Davidsson B. J. R., Skorov Y. V. 2002, On the Light-Absorbing Surface Layer of Cometary Nuclei, I, Radiative Transfer, Icarus, 156, 223

Enzian A. *et al.* 1997, A 2 1/2 D thermodynamic model of cometary nuclei, I, Application to the activity of comet 29P/Schwassmann–Wachmann 1, A&A, 319, 995

Falchi F., Cinzano P., Kyba Ch., Portnov B. 2015, The New World Atlas of Artificial Sky Brightness, IAU Gen. Assemb. 22: 47038F

Fernández J. A. *et al.* 1999, The population, magnitudes, and sizes of Jupiter family comets, A&A, 352, 327

Garstang R. H. 1989, Night-sky brightness at observatories and sites, Astron. Soc. Pac., 101, 306

Gronkowski P. 2007, The search for a cometary outbursts mechanism: a comparison of various theories, Astron. Nachr., 328, 126

Gronkowski P. 2009, Cometary outbursts: the post-deep impact outlook on collisions as possible causes, MNRAS, 397, 883

Gronkowski P., Wesołowski M. 2012, Collisions of comets and meteoroids: the post stardust-NExT discussion, Astron. Nachr., 333, 721

Gronkowski P., Wesołowski M. 2015, A model of cometary outbursts: a new simple approach to the classical question, MNRAS, 451, 3068

Gronkowski P., Wesołowski M. 2016, A Review of Cometary Outbursts at Large Heliocentric Distances, Earth Moon Planets, 119, 23

Gronkowski P., Wesołowski M. 2017, Ejection of large particles from cometary nuclei in the shape of prolate ellipsoids, Astron. Nachr., 338, 385

Gronkowski P., Tralle I., Wesołowski M. 2018, Visibility of comets during their outbursts and the night sky light pollution – Use the Bortle scale, Astron. Nachr., 339, 37

Groussin O., Lamy P., Jorda L. 2004, The nuclei of comets 126P/IRAS and 103P/Hartley 2, A&A, 419, 375

Hughes D. W. (1990) Cometary outbursts: a review, R. Astron. Soc. Q. J., 31, 6

Hughes D. W. 1991, Comet Halley's outburst, MNRAS, 251, 26

Ivanova O. V. *et al.* 2011, Observations of the long-lasting activity of the distant Comets 29P Schwassmann–Wachmann 1, C/2003 WT42 (LINEAR) and C/2002 VQ94 (LINEAR), Icarus, 211, 559

Kossacki K. J., Szutowicz S. 2013, Activity of Comet 29P/Schwassmann–Wachmann 1, Icarus, 225, 111

Montalto M. *et al.* 2008, The comet 17P/Holmes 2007 outburst: the early motion of the outburst material, A&A, 479, L45

Reach W. T. *et al.* (2010) Explosion of Comet 17P/Holmes as revealed by the Spitzer Space Telescope. Icarus, 208: 276

Richardson J. E. *et al.* 2007, A ballistics analysis of the Deep Impact ejecta plume: Determining Comet Tempel 1's gravity, mass, and density, Icarus, 190, 357

Richter N. B. 1954, Die Helligkeitsausbrüche des Kometen 1925 II und ihre Zusammenhänge mit der Sonnentätigkeit, Astron. Nachr., 281, 241

Ściężor T. 2013, A new astronomical method for determining the brightness of the night sky and its application to study long-term changes in the level of light pollution, MNRAS, 435, 303

Tancredi G. *et al.* 2000, A catalog of observed nuclear magnitudes of Jupiter family comets, A&A Suppl., 146, 73

Trigo-Rodriguez J. M. *et al.* 2008a, Outburst activity in comets. I. Continuous monitoring of comet 29P/Schwassmann–Wachmann 1, A&A, 485, 599

Trigo-Rodriguez J. M. *et al.* 2008b, All-Sky Cameras Detection and Telescope Follow-Up of the 17P/Holmes Outburst, Lunar Planetary Science XXXIX, 1627

Trigo-Rodriguez J. M. *et al.* 2010, Outburst activity in comets – II. A multiband photometric monitoring of comet 29P/Schwassmann–Wachmann 1, MNRAS, 409, 1682

Wesołowski M., Gronkowski P. 2018a, A new method for determining the mass ejected during the cometary outburst – Application to the Jupiter-family comets, New Astron., 62, 55

Wesołowski M., Gronkowski P. 2018b, A New Simple Model of Comets-Like Activity of Centaurs, Earth Moon and Planets, 121, 105

Zamorano J., de Sánchez M. A., Ocaña F. *et al.* 2016, Testing sky brightness models against radial dependency: A dense two dimensional survey around the city of Madrid, Spain, J. Quant. Spectrosc. Radiat. Transfer, 181, 52